Proceeding of the IEEE
International Conference on Robotics and Biomimetics
Dali, China, December 2019

Comparison of Different Measurement Matrice for Coded Aperture Snapshot Spectral Imager

Shui Liu[1,2,a], Jixiang Zhang[2,b] , Cui Ma[1,3,c]
And *Hui Lin[1,3,d]

[1]*Shenzhen Institutes of Advanced Technology, Chinese Academy of Sciences, Shenzhen, Guangdong, China*
[2]*China University of Petroleum, Changping, Bejing, China*
[3]*Shenzhen Key Laboratory of Precision Engineering, Shenzhen, Guangdong, China*

[a] shui.liu@siat.ac.cn, [b]zhjx916@163.com,
[c]cui.ma@siat.ac.cn
[d]hui.lin@siat.ac.cn, *Corresponding author

***Abstract* - Multispectral spectral imaging can supply both spatial information and spectral information so it has potential in machine vision. Coded aperture snapshot spectral imager (CASSI) is a fast and compressed multispectral imaging method. The measurement matrice is an indispensable part for signal compression in CASSI, so it greatly influences the quality of the reconstructed signal. In this paper, we mainly analyze and compare several commonly used measurement matrice. The two-step iterative shrinkage/thresholding (TwIST) method is used to reconstruct the multispectral data cube from one encoded image and the peak signal to noise ratio (PSNR) is used to judge the reconstruction quality. The random 0-1 measurement matrice shows the best quality by comparison.**

Index Terms* - *coded aperture snapshot spectral imager ,measurement matrice

I. INTRODUCTION

Imaging spectroscopy is a technique for detecting two-dimensional geometric shapes and one-dimensional spectral information based on targets. It can obtain the continuous spectrum of the object point radiation corresponding to each spatial pixel while acquiring the two-dimensional spatial information of the target object, forming a continuous spectrum image of tens to thousands of bands, forming a data cube arranged in the spectral order. This three-dimensional data obtained by an imaging spectrometer is called a "data cube", as shown in Figure 1. Since the spectral information can be used to identify and classify the target attributes, the two-dimensional image information can provide the spatial distribution characteristics of the target radiation. It is this "combination of the image and spectrum" that makes the imaging spectrometer have extremely high application value in medical imaging [1][2], remote sensing [3], geology [4] and astronomy [5] , robot vision and many other fields.

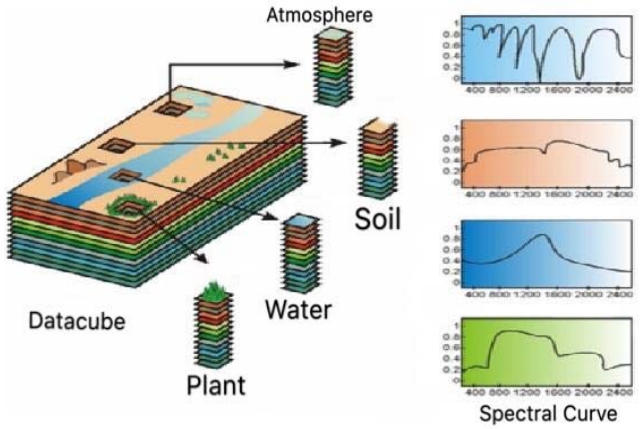

Fig.1 Datacube

The main methods of spectral imaging technology to obtain spectrum information are: spatial point scanning [6], spatial line scanning [7], wavelength scanning [8] and indirect conversion.

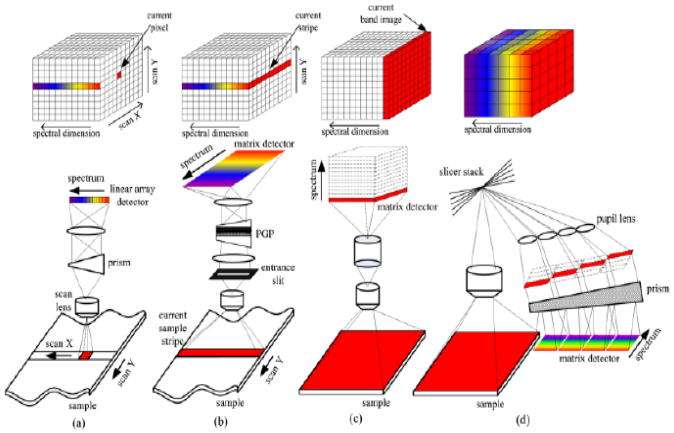

Figure 2 Typical spectral imaging process:a Spot scan;b Line scanning;c Wavelength scanning ; d Indirect transformation

The first three are traditional imaging spectroscopy techniques, and traditional spectroscopy has certain disadvantages:*(i)*data acquisition takes a long time; *(ii)* large amounts of data are acquired and must be stored and transmitted. With the continuous advancement of information technology, people's demand for information is increasing,

978-1-7281-6321-5/19//$31.00 ©2019 IEEE

and the amount of data that needs to be processed and saved is increasing. Therefore, in order to solve the limitations of traditional spectroscopy techniques,spectral imager technology based on compressed sensing [9]-[11] has been proposed [12]-[14], which is an indirect transform. The Coded Aperture Snapshot Spectral Imager (CASSI) [15]-[18] is a popular compression spectroscopy imager that simultaneously captures images at different wavelengths. In CASSI, a three-dimensional data cube can be obtained through two-dimensional information. Therefore, in CASSI, the data values required to be collected are much smaller than those required by conventional imaging spectrometers, which far reduces the required time and speeds up the imaging process.

According to the theory of compressed sensing, three-dimensional data can be reconstructed from two-dimensional data. The theory of compressed sensing mainly includes three aspects: sparse representation, measurement matrice, and reconstruction algorithm. The measurement matrice is an indispensable part for signal compression in CASSI, so it greatly influences the quality of the reconstructed signal. In this paper, we mainly analyze and compare several commonly used measurement matrice. The selection of different measurement matrices has a great influence on the reconstructed signal, so this paper mainly studies the comparison of the performance of different measurement matrice.

II.Coded Aperture Snapshot Spectral Imager

A. *The theory of CASSI*

The coded aperture snapshot spectral imager(CASSI) is a spectral sensing system based on compressed sensing that requires much less data to be collected than traditional imaging spectrometers. In CASSI,(*i*)the 2D spatial information of a scene is coded by an aperture (*ii*)the coded spatial projections are spectrally shifted by a dispersive element, and*(iii)*the coded and shifted projections are detected by a 2D FPA. Suppose we take a scene of spatial dimension M by N and spectral dimension L , the dimension of the image cube is $M \times N \times L$, then the number of measurem λ ents captured by the FPA will be $M(N+L-1)$. In CASSI, the spectral image will be reconstructed from the single image.

B. *The compressed sensing reconstruction*

Fig. 3 is the theory of compressed sensing. When the single is sparse, it can be reconstructed from $\boldsymbol{y}$.

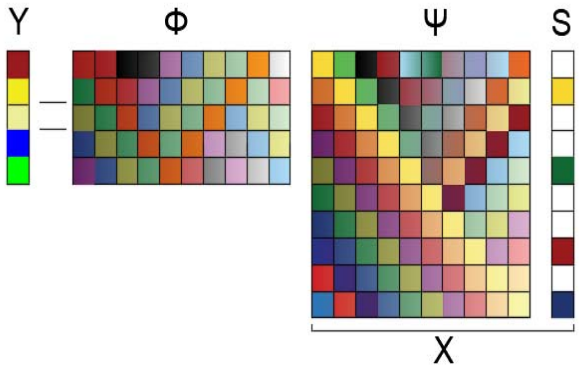

Fig.3 Compressive sensing

$$y = \Phi x, x = \Psi S \rightarrow y = \Phi \Psi S \quad (1)$$

Where $\boldsymbol{x}$ is a signal that satisfies the sparsity (sparse in a certain transform domain); $\boldsymbol{\Phi}$is a measurement matrice. How to solve $\boldsymbol{x}$ under the premise of knowing $\boldsymbol{y}$ is reconstruction algorithm. Compressed sensing problem is to solve $\boldsymbol{x}$ on the basis of known measured values $\boldsymbol{y}$ and $\boldsymbol{\Phi}$. In general, the signal $\boldsymbol{x}$ is not sparse and needs to be a sparse transform. $x = \Psi S$. So the problem is to solve $\boldsymbol{S}$ on the basis of known measured values $\boldsymbol{y}$, $\boldsymbol{\Phi}$ *and* $\boldsymbol{\Psi}$. Therefore, the theory of compressed sensing includes three aspects: sparse representation, measurement matrice, and reconstruction algorithm. Measurement matrice is an indispensable part. It has a direct impact on the reconstruction quality of signal.

Here, the TwIST (Two-step Iterative Shrinkage/Thresholding) is used to reconstruction. It uses the sparsity of spatial gradient. TwIST describes a data cube reconstruction as the solution to the generalized non-linear, unconstrained minimization problem.

$$\hat{f}_{TwIST}(\gamma, T) = [\arg\min_{f}\{\frac{1}{2}\|g - Tf\| + \gamma \bullet TV(f)\}] \quad (2)$$

$$TV(f) = \sum_{k}\sum_{i,j}\sqrt{(f(i+1,j,k)-f(i,j,k))^2 + (f(i,j+1,k)-f(i,j,k))^2} \quad (3)$$

The TV terms penalizes the solution candidates with higher discrete gradients horizontally and vertically.

C. *The peak signal to noise ratio (PSNR)*

The peak signal to noise ratio (PSNR) is used to judge the reconstruction quality.The PSNR is defined as the ratio between the maximum squared value of the ground truth image cube f_0 and the mean square error of the estimatio $\hat{f}$,

$$PSNR = 10log_{10}\left(\frac{max_{x,y,\lambda}\left(f_{0,(x,y,\lambda)}^2\right)}{\sum_{x,y,\lambda}\left(\hat{f}(x,y,\lambda) - f_{0,(x,y,\lambda)}\right)^2}\right) \quad (4)$$

Where $f(x, y, \lambda)$ denotes the element in the cube $\boldsymbol{f}$ at spatial coordinate (x, y) and spectral coordinate λ. f_0 is the initial reference image and $\boldsymbol{f}$ is reconstructed image.

III. MEASURENMENT MATRICE

According to the above analysis, the compressed sensing reconstruction method needs to rely on the measurement matrice. The quality of the measurement matrice directly affects the quality of the reconstruction. This paper mainly studies the effects of different measurement matrice on reconstruction results.

In order to be able to get more information of the original signal from less measurement data, the measurement matrice needs to satisfy the RIP (Restricted Isometry Property). The equivalent condition of RIP is that the sparse representation base is not related to the observation matrice. The RIP property is to ensure that the observation matrice does not map two different sparse signals into the same set.

The matrice we study are Random 0-1 measurement matrice,Gauss measurement matrice ,Bernoulli measurement matrice, Part-Hadamard measurement matrice,Toeplitz measurement matrice and Circulant measurement matrice. The formation of these matrice are briefly introduced.

(i) Random 0-1 matrice is made up of random 0-1 value. Fig. 4 is one pattern with 51×51 pixels.

Fig.4 Random 0-1 coding pattern

(ii) Gauss measurement matrice has a strong randomness. It is composed by gray values.

$$\Phi_{i,j} \sim N(0, \frac{1}{M}) \quad (5)$$

Where M is the numbers of measurements.When $M \rangle cK \log(N/K)$, Gauss measurement matrice will satisfy the RIP.

(iii) Bernoulli measurement matrice has a strong randomness as same as the Gauss matrice. It only includes two different values. So, it is easier to implement and store in practical.

$$\Phi_{i,j} = \begin{cases} +\frac{1}{\sqrt{M}} (P = \frac{1}{2}) \\ -\frac{1}{\sqrt{M}} (P = \frac{1}{2}) \end{cases} = \frac{1}{\sqrt{M}} \begin{cases} +1 (P = \frac{1}{2}) \\ -1 (P = \frac{1}{2}) \end{cases} \quad (6)$$

(iv) Part-Hadamard measurement matrice also satisfies the RIP. First generate a N×N Hadamard matrice, then set M rows from it to form a Part-Hadamard measurement matrice of M×N. It is composed by 1 and -1 values.

(v) T matrice is Toeplitz measurement matrice. C is Circulant measurement matrice. Circulant matrice is a special form of Toeplitz matrice.Where t_n is a random vector.

$$T = \begin{pmatrix} t_n & t_{n-1} & \cdots & t_1 \\ t_{n+1} & t_n & \cdots & t_2 \\ \cdots & \cdots & \cdots & \cdots \\ t_{2n-1} & t_{2n-2} & \cdots & t_n \end{pmatrix} C = \begin{pmatrix} t_n & t_{n-1} & \cdots & t_1 \\ t_1 & t_n & \cdots & t_2 \\ \cdots & \cdots & \cdots & \cdots \\ t_{n-1} & t_{n-2} & \cdots & t_n \end{pmatrix} \quad (7)$$

IV. Simulation results and analysis

To compare the performance of different matrice, a set of spectral images are used for simulation. They are downloaded from the CAVE dataset. Fig.5 is the original RGB image. The dimension of spectral dataset is 512×512×31. It includes 31 wavebands from 400nm to 700nm with an equal spacing of 10nm.

Fig.5 A scene of colorful ballons

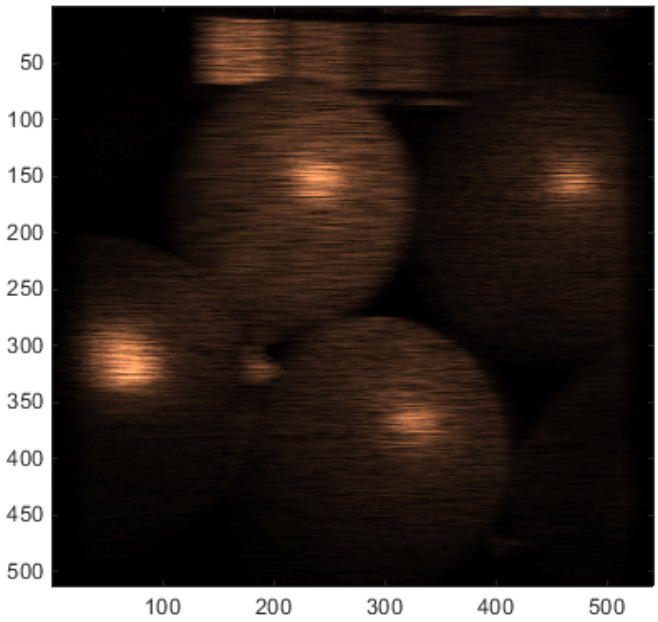

Fig.6 The encoded spectral image

This paper mainly analyzes and compares several commonly used measurement matrice mentioned above, including Random 0-1 measurement matrice , Gauss matrice, Bernoulli matrice, Part-Hadamard, Toeplitz and Circulant matrice. The simulation process is as follows. Firstly, the spectral images are encoded by measurement matrice and combined into one detected image. Fig.6 is one example image using random 0-1 coding matrice. Then, the TwIST method is used to reconstruct the data cube from the single detected image. Finally, PSNR is calculated to quantify the reconstruction quality for different matrice.

Fig.7 shows the simulation results, only several wavelengths are displayed. Fig.7(a) is the original spectral images at 400nm, 500nm, 600nm and 700nm. Fig. 7(b) – Fig. 7(g) are the reconstructed images using random 0-1 matrice, Gauss matrice, Bernoulli matrice, part-Hadamard matrice, Toeplitz matrice and Circulant matrice respectively. From the images, it can be seen that the front three matrices (Random 0-1, Gauss and Bernoulli matrice) are better.

To quantify the difference, the PSNR is calculated between each reconstructed image and original image. As the Table I shows, the PSNR of Random 0-1 and Bernoulli matrice are better and both about 28db. The Gauss matrice follows and 27.3db. The other three matrice are much worse.

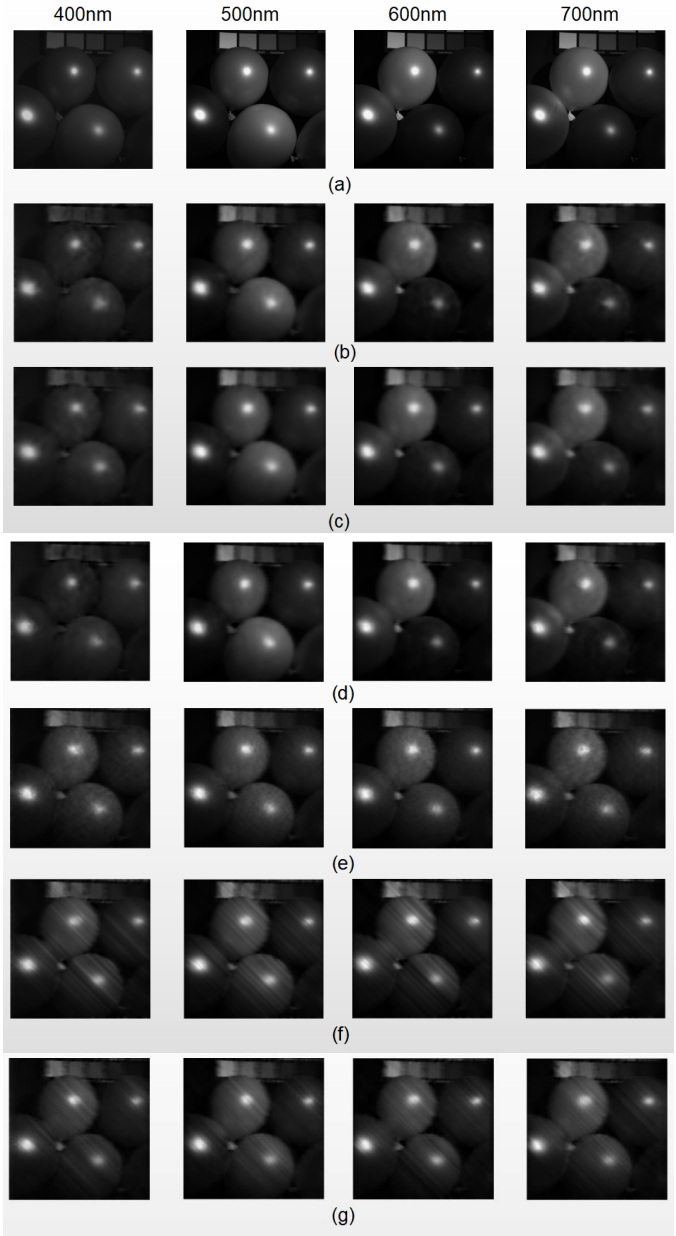

Fig.7 Reconstructed spectral images using compressed sensing with different measurement matrice:(a)original images;(b)Random 0-1 measurement matrice;(c)Gauss measurement matrice ;(d)Bernoulli measurement matrice;(e)PartHadamard measurement matrice;(f)Toeplitz measurement matrice;(g)Circulant measurement matrice

TABLE I
The mean PSNR of different measurement matrice

Measurement matrice	PSNR/db
Random 0-1	28.0044
Gauss	27.3046
Bernoulli	27.9433
Part-Hadamard	23.4814
Toeplitz	23.0167
Circulant	22.6971

To compare the effect on different objects or targets, other two sets of spectral images (object B, object C) are selected for simulation. From TABLE II , the front three matrices are much better than the followed three matrice. It is consistent with the results of Table I. Although the Bernoulli matrice is

better than Random 0-1 matrice for object B, the different is tiny. Therefore, the different measurement matrice have the similar reconstruction performance for different objects.

TABLE II
The mean PSNR on different objects

Measurement matrice	Object A	Object B	Object C
Random 0-1	28.0044	29.7185	29.0052
Gauss	27.3046	29.0147	28.2012
Bernoulli	27.9433	30.0078	28.2435
Part-Hadamard	23.4814	27.1143	24.3218
Toeplitz	23.0167	25.5297	24.0725
Circulant	22.6971	25.1164	23.9875

In experiment, the measurement matrice should be implemented using encoding device, such as the mechanical temple, DMD (Digital Micro-mirror Device). These matrices include 0, 1, -1 and gray values. The 0-1 values are easy to achieve using all of these devices. The -1 value can be achieved by subtracting 1 from 0 which will double measurements. The gray value can be approximated by time lithering which increases time and has biased error. Therefore, both the implementation and performance should be considered in actual application. The random 0-1 matrice would be one good choice.

V. CONCLUSION

This paper makes a comprehensive analysis and comparison about the reconstruction quality of measurement matrices in CASSI. We use the TwIST method to reconstruct the data cube from one encoded image and the PSNR to quantify the reconstruction quality. According to the simulation results, the Random 0-1, Gauss and Bernoulli measurement matrice have similar performance. They are better than part-Hadamard, Toeplitz and Circulant matrice. We will further validate the performance using experiment device in the future.

VI. ACKNOWLEDGMENT

This paper is partially supported by Science and Technology Planning Project of Guangdong Province .

REFERENCES

[1] R. A. Schultz, T. Nielsen, J. R. Zavaleta, R. Ruch, R. Wyatt, and H.R. Garner, “Hyperspectral imaging: A novel approach for microscopic analysis,” Cytometry, vol. 43, no. 4, pp. 239–247, Apr. 2001.

[2] S. V. Panasyuk, S. Yang, D. V. Faller, D. Ngo, R. A. Lew, J. E.Freeman, and A. E. Rogers, “Medical hyperspectral imaging to facilitate residual tumor identifification during surgery,” Cancer Biol.Therapy, vol. 6, no. 3, pp. 439–446, Mar. 2007.

[3] M. E. Schaepman, S. L. Ustin, A. J. Plaza, T. H. Painter, J. Verrelst,and S. Liang, “Earth system science related imaging spectroscopy—Anassessment,” Remote Sens. Environ., vol. 113, pp. S123–S137, Sep.2009.

[4] F. A. Kruse, J. W. Boardman, and J. F. Huntington, “Comparison ofairborne hyperspectral data and EO-1 Hyperion for mineral mapping,”IEEE Trans. Geosci. Remote Sens., vol. 41, no. 6, pp. 1388–1400, Jun.2003.

[5] E. K. Hege, D. O'Connell, W. Johnson, S. Basty, and E. L. Dereniak,“Hyperspectral imaging for astronomy and space surviellance,” in Proc. SPIE's 48th Annu. Meeting Opt. Sci. Technol., Jan. 2004, pp.380–391.

[6] D. J. Brady, Optical Imaging and Spectroscopy. Hoboken, NJ, USA:Wiley, 2009.

[7] M. T. Eismann, Hyperspectral Remote Sensing. Bellingham, WA,USA: SPIE, 2012.

[8] N. Gat, “Imaging spectroscopy using tunable fifilters: A review,” inProc. SPIE, Apr. 2000, vol. 4056, pp. 50–64.

[9] D. Donoho, “Compressed sensing,” IEEE Trans. Inf. Theory, vol. 52,no. 4, pp. 1289–1306, Apr. 2006.

[10] E. Candès, J. Romberg, and T. Tao, “Robust uncertainty principles:Exact signal reconstruction from highly incomplete frequency information,” IEEE Trans. Inf. Theory, vol. 52, no. 2, pp. 489–509, Feb.2006.

[11] R. G. Baraniuk, “A lecture on compressive sensing,” IEEE SignalProcess. Mag., vol. 24, no. 4, pp. 118–121, Jul. 2007.

[12] M. Gehm, R. John, D. Brady, R. Willett, and T. Schulz, “Single-shot compressive spectral imaging with a dual-disperser architecture,” Opt.Exp., vol. 15, no. 21, pp. 14013–14027, Oct. 2007.

[13] X. Yuan, T. Tsai, R. Zhu, P. Llull, D. Brady, and L. Carin, “Compressive hyperspectral imaging with side information,” IEEE J. Sel. Topics Signal Process., vol. 9, no. 6, pp. 964–976, Sep. 2015.

[14] Y. August, C. Vachman, Y. Rivenson, and A. Stern, “Compressive hyperspectral imaging by random separable projections in both the spatial and the spectral domains,” Appl. Opt., vol. 52, no. 10, pp. D46–D54,Mar. 2013.

[15] A. Wagadarikar, N. Pitsianis, X. Sun, and D. Brady, “Spectral image estimation for coded aperture snapshot spectral imagers,” in Proc. SPIE,Sept. 2008, p. 707602.

[16] H. Arguello and G. Arce, “Code aperture optimization for spectrally agile compressive imaging,” J. Opt. Soc. Amer., vol. 28, no. 11, pp.2400–2413, Nov. 2011.

[17] A. Wagadarikar, R. John, R. Willett, and D. Brady, “Single disperser design for coded aperture snapshot spectral imaging,” Appl. Opt., vol.47, no. 10, pp. B44–B51, Apr. 2008.

[18] G. R. Arce, D. J. Brady, L. Carin, H. Arguello, and D. S. Kittle,“Compressive coded aperture spectral imaging: An introduction,”IEEE Signal Process. Mag., vol. 31, no. 1, pp. 105–115, Jan. 2014.